Proceedings of International Conference on Heat Exchanger Fouling and Cleaning - 2013 (Peer-reviewed)
June 09 - 14, 2013, Budapest, Hungary
Editors: M.R. Malayeri, H. Müller-Steinhagen and A.P. Watkinson

Published online
www.heatexchanger-fouling.com

CFD STUDY OF TURBULENCE INDUCED STRUCTURES IN EGR COOLERS

K. Mohammadi and M.R. Malayeri

Institute of Thermodynamics and Thermal Engineering (ITW), University of Stuttgart,
Pfaffenwaldring 6, D-70550 Stuttgart, Germany, m.malayeri@itw.uni-stuttgart.de

ABSTRACT

Exhaust gas recirculation (EGR) coolers can profoundly reduce hazardous NOx emissions from diesel engines. Nevertheless the formation of deposits on EGR surfaces causes design uncertainty and maintenance problems. The present study underlines how changing the EGR surface structure for the same inlet velocity can result in substantial increase in shear stress which otherwise would be needed for an effective deposit suppression. Various structures have been developed then studied numerically using computational fluid dynamics (CFD). The results have been compared with a baseline flat plate rectangular EGR cooler. The numerical findings show that shear stress is increased from 150 to 350% while the overall pressure drop is always below 550 mbar. The geometrical modifications also cause a minor reduction of up to 7% in effective heat transfer area of EGR.

INTRODUCTION

Exhaust gas recirculation (EGR) is a predominantly NOx emission control technology in diesel-engine vehicles. It can either be done internally by simply returning part of exhaust gas to the combustion chamber or externally which is similar to the previous one except the exhaust gas cools down through a cooler known as EGR cooler before returning to the cylinder. Albeit the most common reason for implementing EGR in modern commercial diesel engines is its capability in NOx reduction, its potential application extents to other purposes as well. Advanced combustion concepts under development, e.g. low temperature combustion (LTC), utilize very high EGR rates for emission control. If the application of LTC over a significant portion of the engine operating map becomes commercial, then more demands for EGR systems is anticipated (Junjun et al., 2009; Srinivasan et al., 2010; Zheng et al., 2007).

EGR flow deprives the combustion from a portion of oxygen of the fresh air by introducing cooled exhaust gas, which is lower in oxygen, into the intake system, thereby reducing the combustion temperature and lowering NOx production. However, during the cooling process of EGR, the present soot particles in the exhaust gas form a deposit layer on the EGR walls mainly due to the thermophoresis. The resultant particulate fouling which degrades the heat transfer performance considerably, and therefore, has a profound impact on the design of the EGR coolers (Abd-Elhady et al., 2011a).

Particulate fouling in EGR coolers increases the thermal resistance and consequently deteriorates the cooling efficiency. It is essentially affected by concentration and physical/chemical properties of soot particles, fluid velocity and temperature condition of gas stream and cooler wall, heat capacity rate and temperature of coolant medium, and surface characteristics of EGR walls. Importantly, the net rate of fouling, i.e. the apparent layer formation rate of soot particles on the wall of EGR coolers, is due to the result of competition between two simultaneous mechanisms of deposition and removal/suppression.

In order to keep the cooling performance of the EGR coolers, it is essential to mitigate deposit formation on EGR walls. The possible methods to mitigate the particulate fouling on EGR walls are: the changes in physical/chemical properties of surface of EGR walls in order to hinder the deposition rate (Müller-Steinhagen et al., 2011), and/or to increase the wall shear stress in order to enhance the removal rate of deposition layer (Abd-Elhady et al., 2011b; Müller-Steinhagen et al., 1988; Cabrejos and Klinzing, 1992; Grillot and Icart, 1997). The latter can be achieved by geometrical modification of EGR walls in order to enhance the average value, as well as the manipulating and distribution of fluid flow exerted shear wall through changing fluid velocity.

The main objective of the present study is to develop and analyze geometries which enhance the wall shear stress for different inlet gas velocities. For this purpose, a baseline rectangular EGR cooler will be studied and the distribution of shear wall stress at three different inlet velocities will be attempted. Next, different geometrical modifications will be introduced and the distribution of shear wall stress at the same velocities will be investigated and compared with the results of baseline rectangular EGR cooler. Finally, based on the quality of shear wall stress enhancement, the geometrical modification will be ranked.

DESCRIPTION OF GEOMETRICALLY MODIFIED EGR COOLERS

A flat plate rectangular EGR cooler, shown in Figure 1.a, is considered as the baseline geometry which is referred as EGR01 hereafter. Knowing that the existence of an object confronting the flow will cause instabilities and consequently will develop vortex shedding at certain flow velocities and hence may alter the shear stress, then different structural geometries are considered according to the following criteria:

- Increased average wall shear stress through enhancing flow instabilities or redirection of main flow stream.
- Evenly distribution of effective wall shear stress, i.e. maximize the area where the shear stress is greater than a certain set value. This is, here, considered as the maximum wall shear stress obtained in EGR01).

- Minimization of the ineffective heat transfer area due to the geometrical changes.
- Modification of structure such that the overall pressure drop should be less than a set-limit.
- Minimization of flow dead zones that would otherwise intensify deposition

Figures 1b to 1h, which are referred as EGR02 to EGR08, illustrate the modified geometries. Note that in Figure 1h, angle of attack, AoA, is the angle between the chord line of the wing profile and the vector representing the main stream gas flow in EGR cooler. The direction of main stream gas flow is, in fact, from inlet to outlet of EGR cooler.

CFD METHODOLOGY AND OPERATING CONDITIONS

The prime aim in this study is to augment removal through increased shear stresses by modifying the cooler structure. Therefore, in order to make a consistent comparison between different EGR coolers, air with physical properties of $\rho = 1.225\ kg/m^3$ and $\mu = 1.7894 \times 10^{-5}\ kg/(m.s)$ is considered as working fluid. Moreover no heat transfer is considered for the simulation and instead only fluid mechanics of structurally modified EGR coolers in terms of shear stress and pressure drop have been investigated.

A velocity inlet boundary condition is used to describe the flow conditions at the inlet. Three steady uniform velocities, i.e. 10, 30 and 70 m/s, normal to the inlet are considered which result in Reynolds numbers, Re_{inlet}, ranging from 5,868 to 41,075, respectively. Turbulence intensity $\left(\approx 0.16 Re_{inlet}^{-1/8}\right)$ and length scale $\left(= 0.07 D_{H,inlet}\right)$ characterize the required turbulence parameters at the inlet. Taking into account the possibility of back flow condition at outlet, a rectangular duct with the same geometrical specification of EGR01 is considered as an extension (dummy) immediately next to the outlet of EGR coolers. However, the boundary condition at the outlet of this dummy is defined by specifying the absolute pressure. These types of boundary conditions for inlet and outlet will guarantee the simulation of special flow behavior, e.g. flow separation and vortex shedding which are all important in the present investigation.

The governing equations for mass and momentum conservation are solved numerically using the finite-volume-method-based CFD code of ANSYS-Fluent. A segregated solution method solves the governing equations in implicit formulation sequentially. For the pressure-velocity coupling the SIMPLE algorithm is also applied. The RNG $k - \varepsilon$ model is considered as turbulence model. A standard wall function based on the proposal of Launder and Spalding (1974) bridges the viscosity-affected region between the wall and the fully turbulent region. An examination of the dimensionless sub-layer-scaled distance y^+ showed the correctness of the mesh structure and the use of the introduced semi-empirical function to treat the near wall regions (Fluent, 2008).

It is important to mention that the implemented RNG $k - \varepsilon$ model has a differential formula for effective viscosity which can also describe the effect of swirl on turbulence and complex flow behavior concerning high streamline curvature and strain rate, transitional flows, separated flows as well as vortex shedding, which are very important in the present study. Moreover as the model is, in fact, a two-equation turbulence approach, the numerical calculations of the flow can be converged much faster compared to other turbulence models like Reynolds Stress Model (RSM).

Discretization of geometry and mesh structure

For the description of the flow behavior inside the EGR cooler, mesh structure is developed only for the geometrical fluid domain, e.g. the fluid volume of EGR coolers. For EGR01 to EGR04, the geometrical discretization has been achieved by applying a structured mesh scheme of hexahedral elements. However, for EGR05 to EGR08, i.e. the EGR coolers with sharp-corner ribs, a combination of structured and un-structured mesh schemes have to be used thus a combination of hexahedral and edge shape elements. The aspect ratio of 3D elements is not greater than 2. This will ensure a satisfactory simulation of the isotropic behavior of turbulent flow. Moreover, the skew angle of 3D elements is less than 0.5 which minimizes significantly the numerical errors due to mesh curvature (Ferziger and Perić, 1996; Fluent, 2008).

The above-mentioned mesh scheme will be referred as norm mesh structure. The norm mesh structure was refined about 50% and coarsened about 15% for some EGR coolers, i.e. EGR02 to EGR05. For norm, coarsened and refined mesh structures, the CFD simulations have been carried out for inlet velocities of 10, 30 and 70 m/s. The final results of these simulations have been compared with each other. The comparison showed no significant change in the overall pressure drops by changing the mesh coarsening or refining level. Even for shear wall stress which is more sensitive to mesh resolution, the relative change in wall shear stress due to the mesh refinement or coarsening was less than 1.5%. Moreover, the quality and quantity of flow pattern does not change by variation of the level of mesh coarsening or refining. This ensures the mesh independency of the simulation using the norm mesh structure.

RESULTS AND DISCUSSION

As stated before, the present work attempts to enhance the removal rate of particulate fouling in EGR coolers by stimulating the flow instabilities which would consequently enhance the wall shear stress. This can be achieved by modifying the EGR wall using different turbulence induced structures. However, the introduction of turbulence induced structures in EGR coolers may also increase the overall pressure drop, knowing that the overall pressure drop in EGR coolers should not be greater than 0.1 bar. Table 1 presents the overall pressure drop for all attempted EGR geometries and conditions.

The results presented in Table 1 show that EGR03 to EGR08 generate a pressure drop greater than 0.1 bar, but only at inlet velocity 70 m/s. Knowing that the maximum gas velocity in EGR coolers usually is about 30 m/s (Bravo et al., 2007) and investigating the EGR coolers at gas velocity 70 m/s is only of theoretical interest to discern the behavior of introduced EGRs at very high velocities, Table 1 also shows that all EGR coolers do not generate a pressure drop greater than 0.1 bar for gas velocities, i.e. less than 30 m/s.

Table 1 Overall pressure drop of different EGR coolers.

EGR Geometry	Δp bar u_{inlet} $10\ m/s$	u_{inlet} $30\ m/s$	u_{inlet} $70\ m/s$
EGR01	0.0009	0.0044	0.0185
EGR02	0.0015	0.0087	0.0384
EGR03	0.0119	0.1032	0.5483
EGR04	0.0051	0.0397	0.2050
EGR05	0.0067	0.0508	0.2544
EGR06	0.0044	0.0327	0.1648
EGR07	0.0059	0.0465	0.2329
EGR08	0.0036	0.0295	0.1552

Modifying the EGR rectangular cooler by introducing turbulence induced structures attached on the bottom wall of EGR cooler (see Figures 1a to 1h) could, but not necessarily, decreases the effective heat transfer area and consequently reduce the cooling performance. This would only occur if the attached structures are supposed to be adiabatic or to have very low thermal conductivity due to the possible construction limits. If one considers such scenario then it is important to consider the reduced effective heat transfer area. Table 2 presents the possible reduction in effective heat transfer area of introduced EGR coolers. In Table 2, the base area A_{base} is defined as the area of bottom wall of EGR coolers without the turbulence induced structures (see Figures 1a to 1h).

Table 2 Reduction of effective heat transfer area as a result of seated turbulence inducers.

EGR Geometry	EGR base area, $A_{base}(mm^2)$	$1 - A_{base}/A_{base,EGR01}$
EGR01	6690.00	0.000%
EGR02	6539.60	2.248%
EGR03	6300.00	5.830%
EGR04	6300.00	5.830%
EGR05	6223.62	6.971%
EGR06	6299.87	5.832%
EGR07	6233.92	6.817%
EGR08	6275.75	6.192%

As it is presented in Table 2, the maximum possible reduction in heat transfer area due to the geometrical modification of EGR is less than 7%. Hence, considering the effective heat transfer area, there is no significant difference between the introduced EGR coolers. Now, in order to find the best geometrical modification which may maximize the removal rate of particulate fouling in EGR coolers, the shear stress enhancement has to be evaluated.

The distribution of wall shear stress on the bottom wall of EGR coolers for inlet velocities of 10, 30 and 70 m/s is presented in Figs 2-4. Evidently the maximum wall shear stress is enhanced due to the increase in local fluid velocity. For example, compare the maximum wall shear stress for EGR03 at inlet velocity 10, 30, and 70 m/s with the maximum wall shear stress for other EGR coolers at corresponding inlet velocity. On the other hand, the minimum wall shear stress can be lessened due to the local flow separation or local stagnant flow behind the introduced turbulence induced structures. For example, compare the minimum wall shear stress for EGR03 with the minimum wall shear stress for other EGR coolers at inlet velocity 10, and the same comparison for EGR06 at inlet velocity 30 m/s and for EGR07 at inlet velocity 70 m/s. Although the enhancement in maximum wall shear stress and the reduction in minimum wall shear stress are important for the improvement or deterioration of removal rate, however, these values only may explain the arithmetic mean value of wall shear stress and, in fact, do not explain the distribution of average wall shear stress.

Enhancement in wall shear stress can be compared with the baseline wall shear stress of EGR01. Referring to the distribution of wall shear stress for EGR01 (see Figures 2a, 3a and 4a), the basis wall shear stress τ_{EGR01}^{max} is 2, 8 and 30 pa for inlet velocity 10, 30 and 70 m/s, respectively. For evaluating the distribution of wall shear stress, area $A_{\tau_{wall}>\tau_{EGR01}^{max}}$ is defined as the area where the wall shear stress τ_{wall} is greater than τ_{EGR01}^{max}. Table 3 presents the minimum and maximum wall shear stress, i.e. τ_{wall}^{min} and τ_{wall}^{max}, as well as the absolute and the relative value of $A_{\tau_{wall}>\tau_{EGR01}^{max}}$.

As can be seen in Table 3, some EGR geometries enhance the removal rate of particulate fouling due to the increase of the area with relatively high wall shear stress. For example, for all attempted inlet velocities, EGR05 has the greatest value of $A_{\tau_{wall}>\tau_{EGR01}^{max}}/A_{base}$. On the other hand, other geometries may deliver higher value for arithmetic mean of wall shear stress, e.g. the maximum average wall shear stress at inlet velocities 30 and 70 m/s is obtained in EGR03.

Considering that the overall pressure drop in EGR coolers should be minimized (EGR01, given its flat structure, has the lowest overall pressure drop compared to all attempted geometries), it is essential to introduce a ranking criterion for the evaluation of EGR coolers in which all the important parameters, e.g. the distribution and the average value of wall shear stress and the overall pressure drop, are taken into account. To do so, the dimensionless EGR ranking number $\mathcal{R}_{EGR}$ is defined as:

$$\mathcal{R}_{EGR} = \left(\frac{A_{base}}{A_{norm}}\right)\left(\prod_{j=1}^{n}\left\{\begin{matrix}\left(\frac{\Delta p_{allowable}}{\Delta p_{EGR}}\right)\times\left(\frac{\bar{\tau}_{EGR}}{\tau_{norm}^{max}}\right)\\ \times\left(\frac{A_{\tau_{wall}>\tau_{norm}^{max}}}{A_{base}}\right)\end{matrix}\right\}_{u_{inlet,j}}\right)^{\frac{1}{n}} \quad (1)$$

where $\bar{\tau}_{EGR}$ is the arithmetic mean value of wall shear stress for the corresponding EGR cooler:

$$\bar{\tau}_{EGR} = \frac{\tau_{wall}^{min}+\tau_{wall}^{max}}{2} \quad (2)$$

Although the average wall shear stress should be obtained by applying a surface averaging method, using the arithmetic mean value may ease the calculation of ranking number $\mathcal{R}_{EGR}$. In the present study though, for most cases where the turbulence induced structures are implemented in EGR coolers, the arithmetic averaging of minimum and maximum shear stresses is very close to the surface averaging of wall shear stress, (see the results related to EGR04 to EGR08).

In Eqs (1) and (2), A_{norm} is an arbitrary area which assists the normalization area ratio. Nevertheless in this study, A_{norm} is considered as the base area of EGR01, i.e. $A_{base,EGR01}$. In the meantime, $A_{\tau_{wall}>\tau_{norm}^{max}}$ is the area where the wall shear stress τ_{wall} in an EGR cooler is greater than a basis value for maximum wall shear stress τ_{norm}^{max}, $\Delta p_{allowable}$ is the allowable maximum pressure drop in EGR coolers due to the operational limitation, and Δp_{EGR} is the overall pressure drop in EGR cooler. Index $u_{inlet,j}$ refers to the aforementioned values for various inlet velocities and n is the number of attempted velocities. For the calculation of Eq. (1), $\Delta p_{allowable}$ is set to be an arbitrary value equal to 0.1 bar, τ_{norm}^{max} is equal to τ_{EGR01}^{max}, and $n = 3$ ($u_{inlet,1} = 10\ m/s$, $u_{inlet,2} = 30\ m/s$, $u_{inlet,3} = 70\ m/s$). Table 4 presents the ranking number $\mathcal{R}_{EGR}$ for all structured EGR coolers investigated in this study.

Table 3 τ_{wall}^{max}, τ_{wall}^{min} and absolute and relative value of $A_{\tau_{wall}>\tau_{EGR01}^{max}}$ for different EGR coolers at three inlet velocities.

	$u_{inlet} = 10\ m/s$, $\tau_{EGR01}^{max} = 2\ pa$			
EGR Geometry	$\tau_{wall}^{min}\ (pa)$	$\tau_{wall}^{max}\ (pa)$	$A_{\tau_{wall}>\tau_{EGR01}^{max}}\ (mm^2)$	$A_{\tau_{wall}>\tau_{EGR01}^{max}}/A_{base}$
EGR01	0.2019	1.8114	0.00	0.00%
EGR02	0.0326	3.0958	69.76	1.07%
EGR03	0.0113	4.4303	672.28	10.67%
EGR04	0.0115	3.5444	1346.33	21.37%
EGR05	0.0568	4.2347	2340.49	37.61%
EGR06	0.0471	3.1008	776.56	12.33%
EGR07	0.0561	3.6670	1568.32	25.16%
EGR08	0.0328	4.5106	1335.81	21.29%

	$u_{inlet} = 30\ m/s$, $\tau_{EGR01}^{max} = 8\ pa$			
EGR Geometry	$\tau_{wall}^{min}\ (pa)$	$\tau_{wall}^{max}\ (pa)$	$A_{\tau_{wall}>\tau_{EGR01}^{max}}\ (mm^2)$	$A_{\tau_{wall}>\tau_{EGR01}^{max}}/A_{base}$
EGR01	1.1363	7.4364	0.00	0.00%
EGR02	0.2359	16.7825	208.90	3.19%
EGR03	0.1207	24.9688	1525.76	24.22%
EGR04	0.1951	21.8330	2574.41	40.86%
EGR05	0.1801	21.1146	4130.61	66.37%
EGR06	0.1087	15.9511	3169.08	50.30%
EGR07	0.1181	19.2731	3673.78	58.93%
EGR08	0.5147	23.8776	3967.20	63.21%

	$u_{inlet} = 70\ m/s$, $\tau_{EGR01}^{max} = 30\ pa$			
EGR Geometry	$\tau_{wall}^{min}\ (pa)$	$\tau_{wall}^{max}\ (pa)$	$A_{\tau_{wall}>\tau_{EGR01}^{max}}\ (mm^2)$	$A_{\tau_{wall}>\tau_{EGR01}^{max}}/A_{base}$
EGR01	4.7786	27.9043	0.00	0.00%
EGR02	0.6724	65.6373	322.96	4.94%
EGR03	0.4661	113.0447	1747.29	27.73%
EGR04	0.9875	100.5810	2747.59	43.61%
EGR05	0.7686	87.8075	4608.62	74.05%
EGR06	0.6541	65.2011	4003.54	63.55%
EGR07	0.4584	77.6941	4237.28	67.97%
EGR08	2.9603	99.4638	4560.83	72.67%

Table 4 Ranking number $\mathcal{R}_{EGR}$ for all attempted EGR geometries.

EGR Geometry	$\mathcal{R}_{EGR}$	Ranking Position
EGR01	0.00	7
EGR02	0.31	6
EGR03	0.31	6
EGR04	1.17	4
EGR05	1.54	2
EGR06	1.06	5
EGR07	1.23	3
EGR08	2.44	1

Based on the analysis summarized in Table 4, the most effective EGR geometry for enhancing the wall shear stress and consequently the removal rate is EGR08. EGR05 and EGR07 are in the second and third ranking list. Concerning EGR08, the enhancement in wall shear stress is profound when it is compared with the flat rectangular EGR cooler, i.e. EGR01. The average wall shear stress in EGR01 is about 1, 4.3, and 16.3 pa at inlet velocity 10, 30 and 70 m/s, respectively. However, the corresponding wall shear stresses for EGR08 are about 2.3, 12.2 and 51.2 pa. These wall shear stresses can be achieved in EGR01 at inlet velocities 25, 55, and 125 m/s, correspondingly. These corresponding inlet velocities are equal to the critical velocities in the baseline EGR rectangular coolers that are required for removing soot particles in the size of about 0.75 μm, 0.2 μm, and 50 nm (Abd-Elhady et al., 2011b).

CONCLUDING REMARKS

The present investigation demonstrates the possibility of modifying EGR cooler geometries by introducing turbulence induced structures which may increase the flow instabilities and consequently enhance the wall shear stress. This would, in turn, give rise to increased deposit removal from the surface of the EGR cooler. The enhancement in wall shear stress is significant compared to that of a flat rectangular EGR cooler. For the ranking of EGR coolers a new dimensionless ranking number $\mathcal{R}_{EGR}$ is also defined which considers all important parameters required for the appraisal of various EGR coolers in terms of hydrodynamics.

Comparison of different EGR coolers shows that the best geometry is the EGR rectangular cooler with 7 conventional wings similar to NACA-Profile 6412 with angle of attack 38°, i.e. EGR08. The average wall shear stress obtained in EGR08 at inlet velocity 10, 30 and 70 m/s corresponds to average wall shear stress in EGR01 which can be obtained at inlet velocity 25, 55 and 125 m/s. These correspond to the critical removal velocities required for removing soot particles of about 0.75 μm, 0.2 μm, and 50 nm.

Nomenclature

A	Area, mm^2
AoA	Angle of attack
D_H	Hydraulic diameter, m
k	Kinetic energy of turbulence fluctuations per unit mass, m^2/s^2
n	Number of attempted inlet velocities, $-$
Re	Reynolds number, $-$
$\mathcal{R}_{EGR}$	EGR ranking number, $-$
u	Fluid velocity, m/s

Greek symbols

Δp	Overall pressure drop, bar
ε	Dissipation rate of kinetic energy of turbulence fluctuations per unit mass, m^2/s^3
μ	Fluid dynamic viscosity, $kg/(m.s)$
ρ	Fluid density, kg/m^3
τ	Wall shear stress, N/m^2

Mathematical symbols and operators

$\overline{}$	Arithmetic average value
Π	Mathematical symbol for the product of a sequence of terms

Subscripts

$allow$	Maximum allowable value
$base$	Related to the base area of EGR cooler
EGR	Related to the values for a certain EGR cooler
$EGR01$	Related to the values for a EGR01
j	Refers to the value at the attempted inlet velocity j
$inlet$	Refers to the condition at the inlet
$norm$	Refers to a basis value
$wall$	Refers to the conditions or values at EGR wall
$\tau_{wall} > \tau_{norm}^{max}$	Related to a value where the wall shear stress τ_{wall} is greater than a basis value of maximum wall shear stress τ_{norm}^{max}
max	Maximum value
min	Minimum value

REFERENCES

Abd-Elhady, M.S., Malayeri, M.R. and H. Müller-Steinhagen, 2011a, Fouling problems in exhaust gas recirculation coolers in the automotive industry, Heat Transfer Eng., Vol. 32, Nos. 3-4, pp. 248-257.

Abd-Elhady, M.S., Zornek, T., Malayeri, M.R., Balestrino, S., Szymkowicz, P.G. and Müller-Steinhagen, H., 2011b, Influence of gas velocity on particulate fouling of exhaust gas recirculation coolers, Int. J. Heat and Mass Transfer, Vol. 54, pp.838-846.

Bravo, Y., Moreno, F., Longo, O., 2007, Improved Characterization of Fouling in Cooled EGR Systems, Society of Automotive Engineers Technical Paper Series, No. 2007-01-1257.

Cabrejos, F. J., Klinzing, G. F., 1992, Incipient Motion of Solid Particles in Horizontal Pneumatic Conveying, Powder Technology, Vol. 72, Issue 1, pp. 51-61.

Ferziger, J. H., Perić, M., 1996, Computational Methods for Fluid Dynamics, Springer-Verlag, Berlin.

FLUENT Incorporated, 2008, “Fluent 6.3, User’s Guide”, Fluent Incorporated.

Grillot, J. M., Icart, G., 1997, Fouling of a Cylindrical Probe and a Finned Tube Bundle in a Diesel Exhaust

Environment, Experimental Thermal and Fluid Science, Vol. 14, Issue 4, pp. 442-454.

Jacobs, E. N., Ward, K. E., Pinkerton, R. M., 1933, The Characteristics of 78 Related Airfoil Sections From Tests in the Variable-Density Wind Tunnel, Naca-Report-460.

Jang, S., Park, S., Choi, K., Kim, H., 2011, Experimental Investigation of the Influences of Shape and Surface Area on the EGR Cooler Efficiency, Vo. 47, Issue 6, pp. 621-628.

Junjun, Z., Xinqi, Q., Zhen, W., Bin, G., Zhen, H., 2009, Experimental Investigation of Low-Temperature Combustion (LTC) in an Engine Fueled with Dimethyl Ether (DME), Energy & Fuels, Vol. 23, Issue 1, pp. 170-174.

Launder, B. E., Spalding, D. B., 1974, The Numerical Computation of Turbulent Flows, Computer Methods, in “Applied Mechanics and Engineering”, Vol. 3, Issue 2, pp. 269-289.

Müller-Steinhagen, H., Reif, F., Epstein, N., Watkinson, P., 1988, Influence of Operating Conditions on Particulate Fouling, Canadian Journal of Chemical Engineering, Vol. 66, Issue 1, pp. 42-50.

Müller-Steinhagen, H., Malayeri, M.R. and Watkinson, A.P., 2011, Heat exchanger fouling: Cleaning and mitigation techniques, Heat Transfer Eng., Vol. 32, Nos. 3-4, pp. 189-196.

Park, S., Choi, K., Kim, H., Lee, K., 2010, Influence of PM Fouling on Effectiveness of Heat Exchanges in a Diesel Engine with Fin-Type EGR Coolers of Different Sizes, Vol. 46, Issue 11-12, pp. 1221-1227.

Srinivasan, K. K., Mago, P. J., Krishnan, S. R., 2010, Analysis of Exhaust Waste Heat Recovery from a Dual Fuel Low Temperature Combustion Engine using an Organic Rankine Cycle, Vol. 35, Issue 6, pp. 2387-2399.

Zheng, M., Mulenga, M. C., Reader, G. T., Wang, M., Ting, D. S-K., Tjong, J., 2007, Biodiesel Engine Performance and Emissions in Low Temperature Combustion, Vol. 87, Issues 6, pp. 714-722.

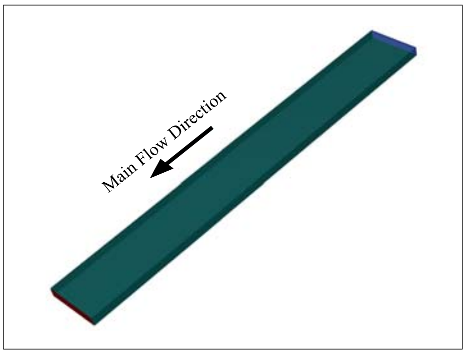

Figure 1a: EGR rectangular cooler (EGR01), 223 mm long × 30 mm wide × 5 mm thick.

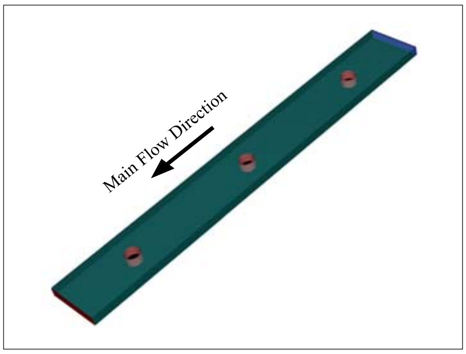

Figure 1b: EGR rectangular cooler with 3 in-lined cylinders (EGR02). The cylinders are 8 mm in diameter and 5 mm long.

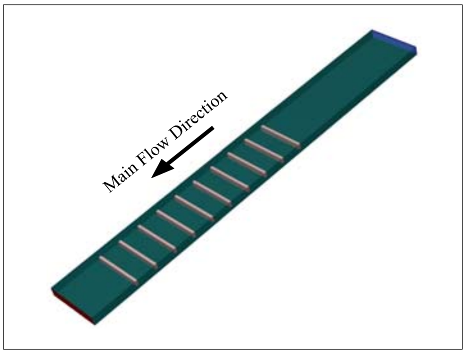

Figure 1c: EGR rectangular cooler with straight ribs (EGR03). The ribs are arranged vertically with respect to inlet flow direction and are 26 mm long and 3 mm wide and have a thickness of 1.5 mm.

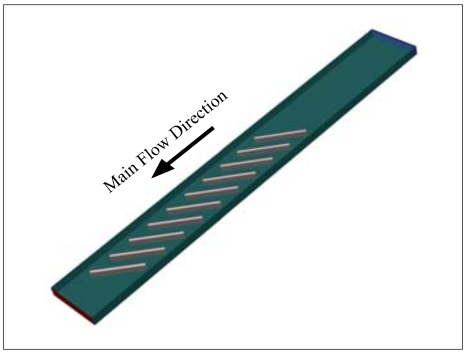

Figure 1d: EGR rectangular cooler with straight ribs (EGR04). The ribs are arranged 135° inclined with respect to inlet flow direction and are 26 mm long and 3 mm wide and have a thickness of 1.5 mm.

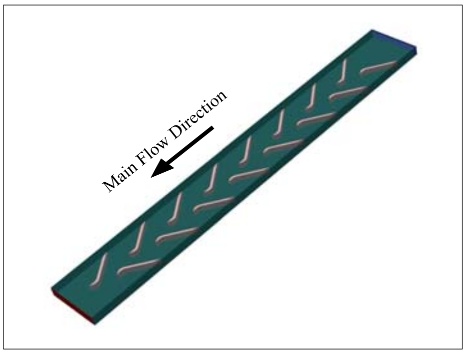

Figure 1e: EGR rectangular cooler with curvy form ribs (EGR05). The ribs are arranged 135° inclined with respect to inlet flow direction. They are 20.5 mm long and 3 mm wide and have a thickness of 1.5 mm. The rib-side wall gap is 2.75 mm.

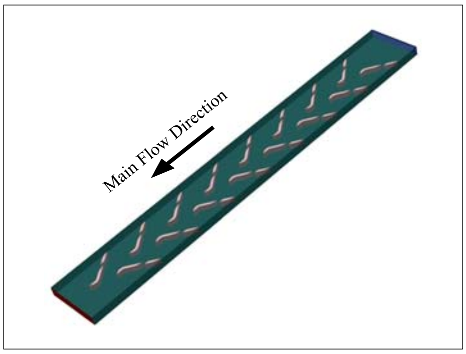

Figure 1f: EGR rectangular cooler with curvy form ribs (EGR06). This geometry is similar to EGR05; however, a small channel is contrived is each rib. This channel is 1.69 mm wide and is located in the $^{9}/_{28}$ of the length of rib.

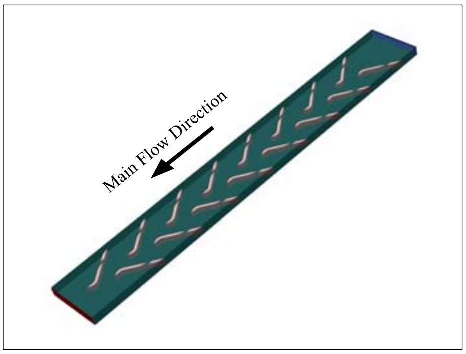

Figure 1g: EGR rectangular cooler with curvy form ribs (EGR07). This geometry is similar to EGR06; however, the small channel is 1.37 mm wide and is located in the $^{10}/_{28}$ of the length of rib. Moreover, the rib-side wall gap is 1.37 mm.

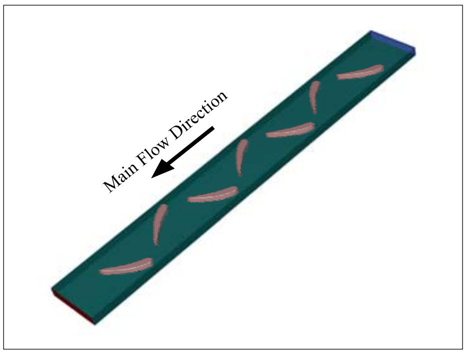

Figure 1h: EGR rectangular cooler with 7 conventional wings (EGR08). The wings are very similar to NACA-Profile 6412. The maximum wing thickness is 3.78 mm and the chord length is 24.11 mm. The wings are 2.5 mm long with angle of attack, or AoA, 38°.

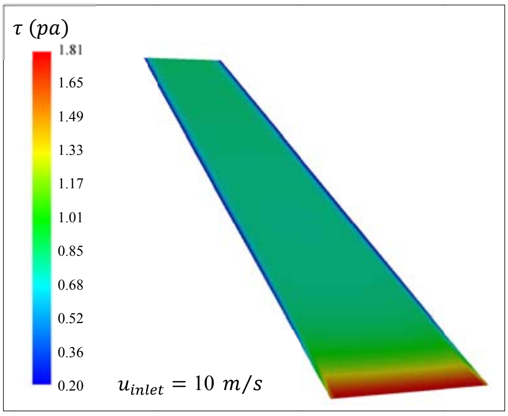

Figure 2a: The distribution of wall shear stress for EGR01.

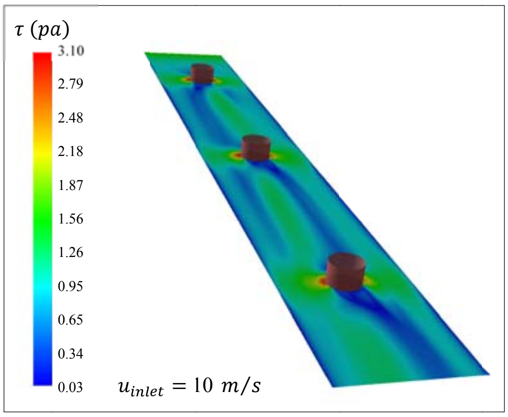

Figure 2b: The distribution of wall shear stress for EGR02.

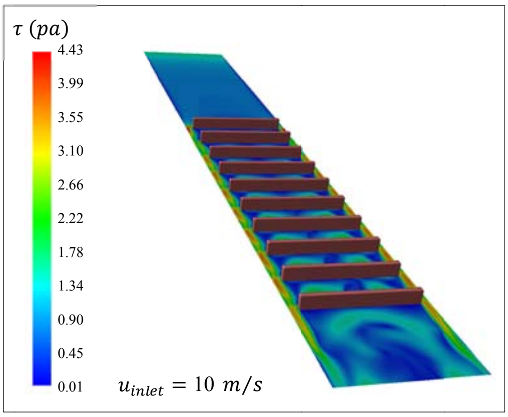

Figure 2c: The distribution of wall shear stress for EGR03.

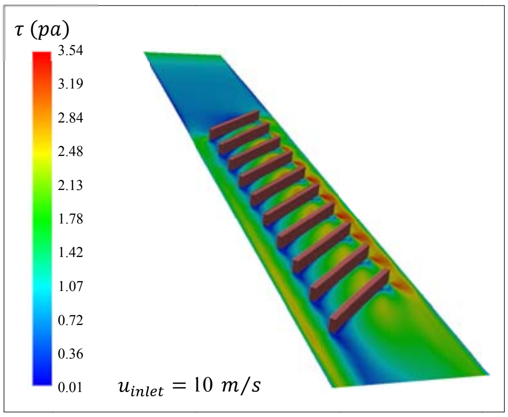

Figure 2d: The distribution of wall shear stress for EGR04.

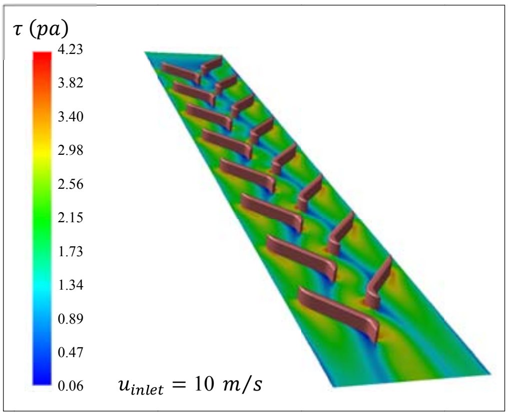

Figure 2e: The distribution of wall shear stress for EGR05.

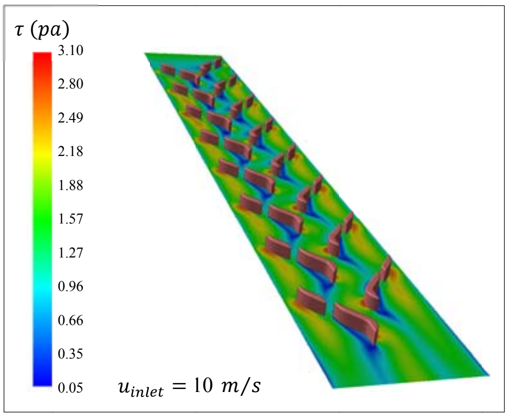

Figure 2f: The distribution of wall shear stress for EGR06.

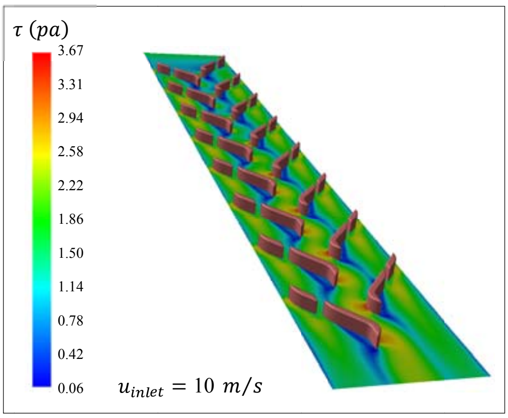

Figure 2g: The distribution of wall shear stress for EGR07.

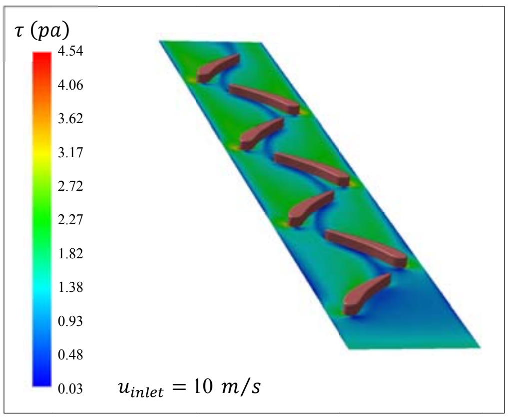

Figure 2h: The distribution of wall shear stress for EGR08.

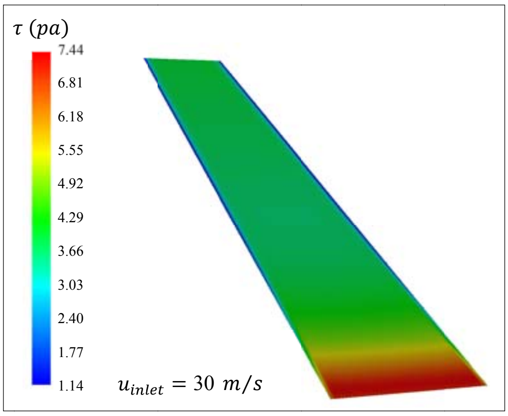

Figure 3a: The distribution of wall shear stress for EGR01.

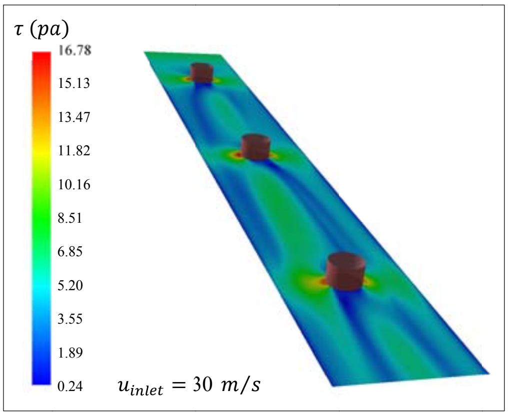

Figure 3b: The distribution of wall shear stress for EGR02.

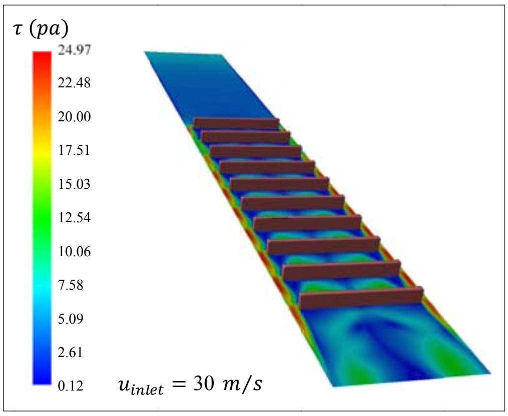

Figure 3c: The distribution of wall shear stress for EGR03.

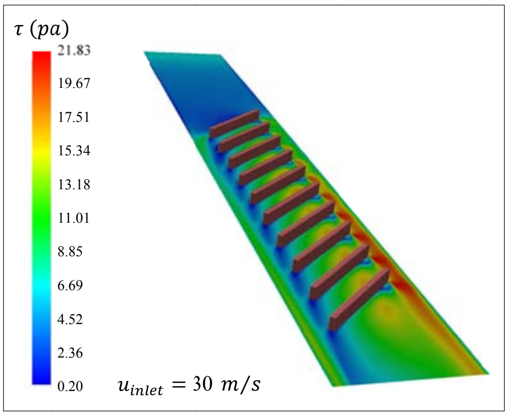

Figure 3d: The distribution of wall shear stress for EGR04.

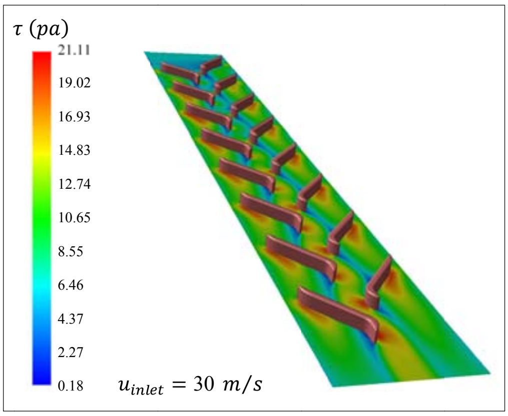

Figure 3e: The distribution of wall shear stress for EGR05.

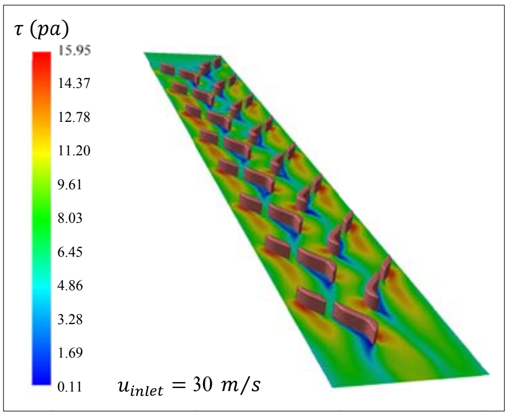

Figure 3f: The distribution of wall shear stress for EGR06.

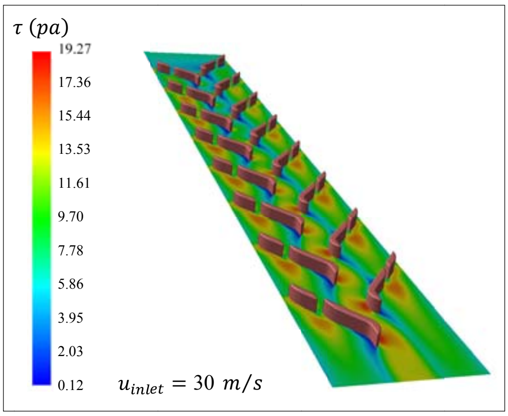

Figure 3g: The distribution of wall shear stress for EGR07.

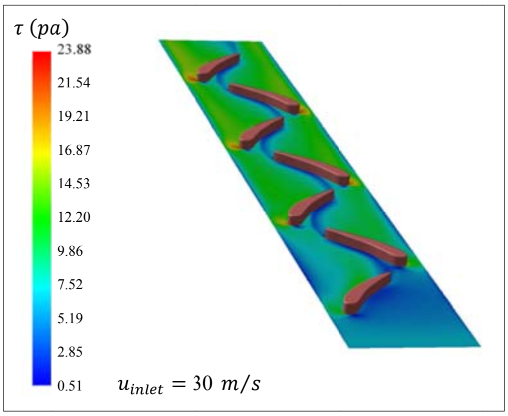

Figure 3h: The distribution of wall shear stress for EGR08.

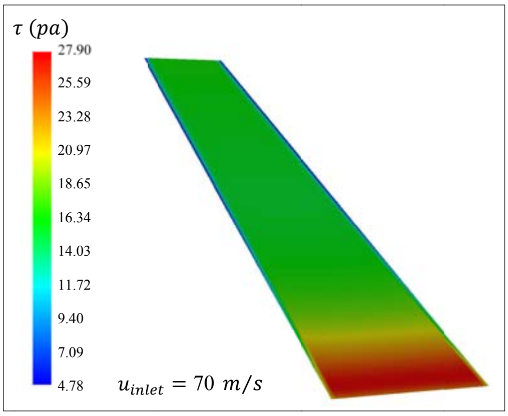

Figure 4a: The distribution of wall shear stress for EGR01.

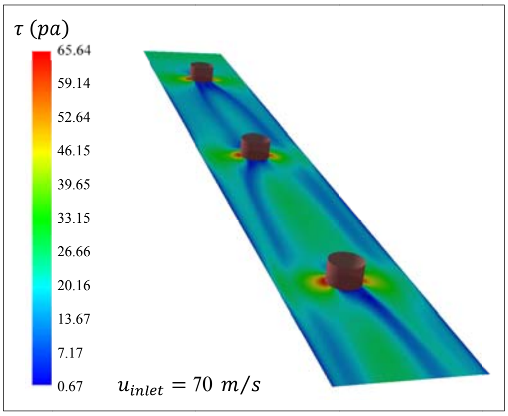

Figure 4b: The distribution of wall shear stress for EGR02.

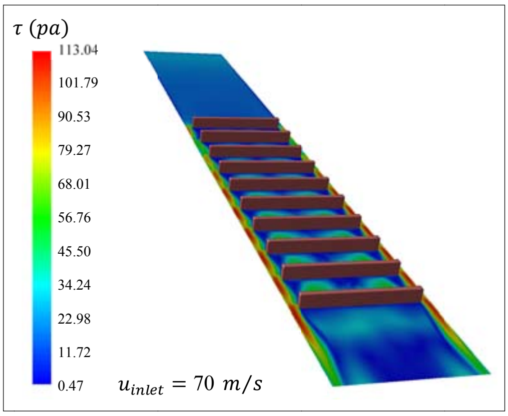

Figure 4c: The distribution of wall shear stress for EGR03.

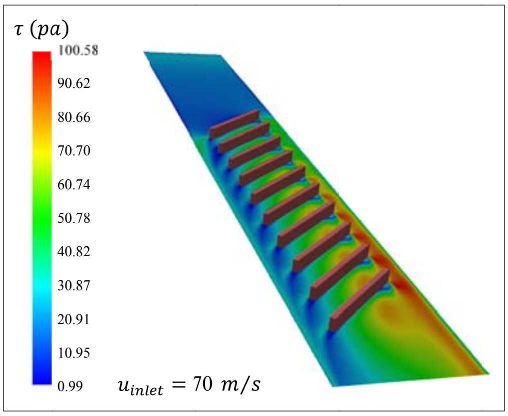

Figure 4d: The distribution of wall shear stress for EGR04.

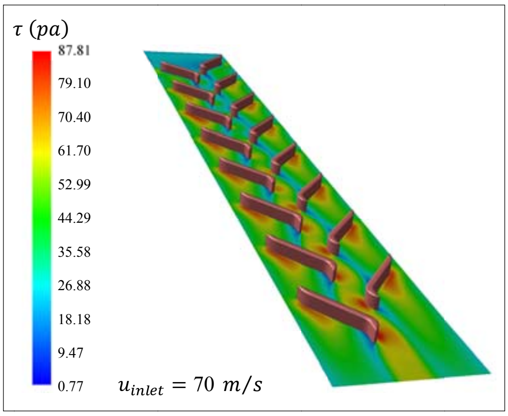

Figure 4e: The distribution of wall shear stress for EGR05.

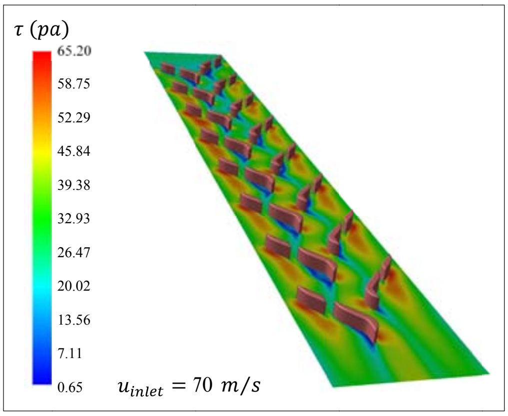

Figure 4f: The distribution of wall shear stress for EGR06.

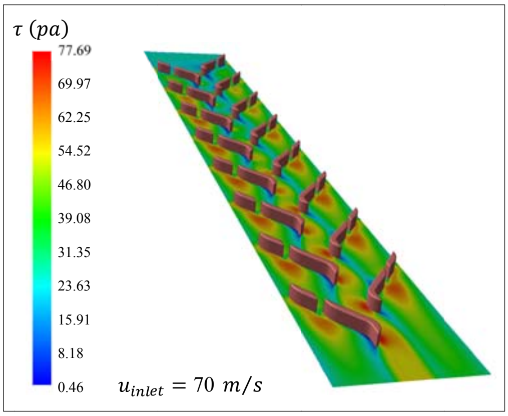

Figure 4g: The distribution of wall shear stress for EGR07.

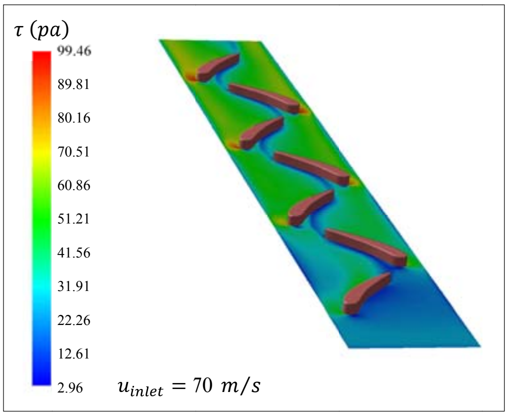

Figure 4h: The distribution of wall shear stress for EGR08.